Supercritical CO_2 Brayton power cycles for DEMO fusion reactor based on Helium Cooled Lithium Lead blanket

José Ignacio Linares[a], Luis Enrique Herranz[b], Iván Fernández[b], Alexis Cantizano[a], Beatriz Yolanda Moratilla[a]

[a] Comillas Pontifical University, Alberto Aguilera, 25, 28015 Madrid, Spain
[b] CIEMAT, Complutense, 40, 28040 Madrid, Spain

ABSTRACT

Fusion energy is one of the most promising solutions to the world energy supply. This paper presents an exploratory analysis of the suitability of supercritical CO_2 Brayton power cycles (S-CO_2) for low-temperature divertor fusion reactors cooled by helium (as defined by EFDA). Integration of three thermal sources (i.e., blanket, divertor and vacuum vessel) has been studied through proposing and analyzing a number of alternative layouts, achieving an improvement on power production higher than 5% over the baseline case, which entails to a gross efficiency (before self-consumptions) higher than 42%. In spite of this achievement, the assessment of power consumption for the circulating heat transfer fluids results in a penalty of 20% in the electricity production. Once the most suitable layout has been selected an optimization process has been conducted to adjust the key parameters to balance performance and size, achieving an electrical efficiency (electricity without taking into account auxiliary consumptions due to operation of the fusion reactor) higher than 33% and a reduction in overall size of heat exchangers of 1/3. Some relevant conclusions can be drawn from the present work: the potential of S-CO_2 cycles as suitable converters of thermal energy to power in fusion reactors; the significance of a suitable integration of thermal sources to maximize power output; the high penalty of pumping power; and the convenience of identifying the key components of the layout as a way to optimize the whole cycle performance.

1. Introduction

Fusion energy is one of the most promising solutions to the world energy problem. Among its most outstanding features are intrinsic safety, management of environmental impact, and long-term availability of primary fuels (deuterium, lithium). In sight of such a potential, the European Commission requested EFDA (European Fusion Development Agreement) to prepare a technical roadmap to achieve fusion electricity by 2050 [1]. On the way, there will be two major cornerstones: ITER (International Tokamak Experimental Reactor) and DEMO (DEMOnstration Power Plant). ITER shall demonstrate the technological feasibility of fusion energy by producing net energy (the ratio between net electricity to heating and current drive energy supply greater or equal to ten) and by testing key technologies for the following steps towards commercial fusion power plants [2]. DEMO will constitute the intermediate stage between ITER and fusion power plants. It shall demonstrate the integrated operation of the necessary technologies for net power production at pre-commercial level. The selection of DEMO design must start from a rigorous review of the existing options. It is at this early stage when all the

design criteria should be accounted for, cost and robustness included. This is a must for fusion technology entry in the energy market, as it will strongly depend on its competitiveness. The main factors affecting the cost of fusion energy (by increasing reactor availability and reducing investment and operation costs) are clearly identified [1], as power conversion cycles, where efficiency might affect considerably. The design of the power conversion cycle will also affect the choice of breeding blanket coolants and materials. As a consequence, the EFDA strategy includes a program for Balance of Plant (BoP) modeling, analysis and evaluation, so that appropriate engineering tools are developed and industry gets involved. Furthermore, a research and development activity will be launched to address challenging issues like tritium control in heat exchangers, response to cyclic operation and BoP components failure modes.

The breeding blanket is the main thermal source for the power conversion cycle in a fusion reactor. Depending on its cooling medium four types of blankets are distinguished: Water Cooled Lithium Lead (WCLL), Helium Cooled Lithium Lead (HCLL), Dual Cooled Lithium Lead (DCLL) and Self Cooled Lithium Lead (SCLL). The second thermal source in order of importance is the divertor, a device devoted to collect the plasma waste. This thermal source can operate at high (above 500 °C) or low temperature (below 250 °C), depending on the coolant medium (helium for high and water for low temperature). Finally, the vacuum vessel cooling can also supply heat to the conversion power cycle, although in the lowest temperature and power range [3].

In the EFDA Work Programme 2013 different solutions for power conversion system at DEMO were analyzed [4]. The Brayton cycle is very attractive due to its relative simplicity and compactness. However, use of a very light gas (i.e., Helium) taxes thermal efficiency because of the necessary compression before absorbing heat from the thermal source. This might be partially compensated by using thermal recuperation and by reaching very high temperatures. A good example for these two strategies are the so called VHTRs fission reactors [5], in which temperatures as high as $900 \div 1000$ °C are postulated. Unfortunately, fusion reactors do not reach so high thermal levels, even at high temperature divertors [6]. In the particular case of supercritical carbon dioxide (S-CO_2), Brayton cycles overcome the high demand of compression power by entering the compression stage at a pressure slightly higher than the critical one, so that specific volume is not as large as if it was an ideal gas. Dostal compiled the fundamentals of the cycle and deepened in its performance, including heat exchanger designs, economy and turbomachinery [7]. The most outstanding feature of S-CO_2 cycles with respect to Rankine ones is probably their remarkable compactness. Other characteristics, though, are less favorable. Precooling, for instance, is rather complex. If the cycle low pressure is near the critical one (typically 75 bar), CO_2 specific heat experiences a very sharp peak at low temperatures that makes heat transfer intricate. Additionally, such low pressures mean heat rejection at very low temperature differences, which requires high water flow rates (i.e., much pumping power) at the secondary side of the heat exchanger.

Most papers on S-CO_2 Brayton cycles deal with Generation IV fission plants, especially with Sodium Fast Reactors (SFR). High temperature thermal sources of SFRs [8] are comparable to those of DEMO with the HCLL blanket [4], so some literature about this type of fission reactors has been revised. Dostal et al. [9] explored different configurations with Brayton cycles using CO_2, from basic ones to re-compression cycles, pre-compression and partial cooling compression cycles. They concluded re-compression has the potential to achieve high efficiencies (higher than 46%), but the value of pressure should be over 200 bar for a significant result. A study conducted under similar conditions to the DEMO blanket ones concluded that no efficiency increase should be expected from

inter-cooling and/or re-heating with respect to the re-compression cycle [10]. Second law analyses of the re-compression cycle were carried out to find out the potential effect of different parameters on the exergetic efficiency [11]. Finally, other studies focused on enhancing cycle efficiencies through using binary gas mixtures [12].

The DEMO is well framed in the low temperature divertor family. A comparative analysis was conducted regarding both blanket coolant and power cycle configurations for a fusion reactor [13]. Helium proved to be better than pressurized or supercritical water due to its stability. Among steam Rankine, He-Brayton and S-CO_2 cycles, the analysis results depended on how blanket and divertor were considered. When both components were jointly considered as thermal sources, the highest efficiency was Rankine's, closely followed by S-CO_2. However, if the blanket was conceived as the only thermal source, the Rankine reversed and S-CO_2 got the highest efficiency, closely followed by Rankine. Inclusion of the divertor was calculated to heavily tax S-CO_2 cycle efficiency (from 42% to 36.4%), but it allows generating further net power. Finally, a design including size of components was performed giving a gross volume of 16,590 m^3 (87% for heat exchangers) for steam power plant against 7240 m^3 (83% for heat exchangers) for S-CO_2.

The key of the S-CO_2 Brayton cycle is the situation of the main compressor suction close to the critical point, which allows achieving a low compressor consumption. The feasibility of the cycle depends on the stability of the compressor when operating close to the critical point, and even when operation conditions fall below the dome region of the saturation curve. This issue has been studied by the SANDIA laboratory. They released a report [14] in 2010 explaining the test loops and showing exhaustive experimental results. These experimental results demonstrated stable and controllable operation near the critical point over a range of conditions and confirmed the performance potential of S-CO_2 cycles. Another issue about the operation close to critical point is the sharp variation of density of the CO_2, being this topic studied by Moisseytsev and Sienicki [10]. So, when the compressor inlet temperature is below the pseudocritical temperature (the one at the peak in the specific heat occurs) the density is very high, reducing the compressor consumption. However, it is necessary to control this temperature because at pressures slightly higher than the critical one (around 74 bar) a small increase in this temperature produces a sharp drop in the density, with the associate problem in the operation of the compressor. This fact can be smoothed if the compressor inlet pressure is increased enough. With regards to turbomachinery design for CO_2, SANDIA Laboratories synthesized in Ref. [15] some orientations. A more detailed explanation can be found in Ref. [16].

One of the challenges of any power conversion system in a fusion power plant is to accommodate a pulsed mode operation. In order to discuss how S-CO_2 cycles would behave, concentrated solar plants (CSP) are taken as a reference given the natural cycling of their power source, where a thermal energy storage system (TES) is usually proposed to extend the operating hours of the plant. An optimization study can be found in Ref. [17]. Supercritical CO_2 power conversion systems are being proposed for CSP, especially for the central tower system. A thorough description is given in Refs. [18], where it proposed molten salt as a thermal energy storage system. In Ref. [19] advanced layouts based on S-CO_2 cycles are proposed for CSP plants, including combined cycles using organic Rankine cycles as bottoming cycles. SunShot Project promoted by the Department of Energy of USA seeks to develop a megawatt-scale S-CO_2 cycle optimized for the highly transient solar power plant profile [20]. Also, some tests conducted in SANDIA laboratories concluded S-CO_2 cycles are well adapted to transient behavior due to the short solar oscillations along a day and their low thermal mass, whereas TES might

be used to overcome longer oscillations [21]. In Ref. [22] the control strategies for CSP power plants (trough and tower) are discussed for daily fluctuations. In the nuclear sector Floyd et al. [23] dealt with the off-design response of S-CO_2 cycles when the sink temperature varies in the conversion power plant of an SFR nuclear power plant. Different control strategies for stability of the system are assessed.

The Printed Circuit Heat Exchanger (PCHE) is a rather novel heat exchanger type, formed by diffusion bonding of a stack of plates with fluid passages photo-chemically etched on one side of each plate by using a technique derived from that employed for electronic printed circuit boards–hence the name. The diffusion bonding process allows getting an interface-free joint between the plates, giving strength to the base material and very high pressure containment capability. The use of such heat exchangers has been investigated by Aquaro et al. [24] for high temperature recuperators in Brayton power plants (air and helium, not supercritical CO_2) in fossil and VHTR fission power applications. They conclude that in this context (high temperature and not so high pressure) other compact heat exchangers, as plate-fin ones, or shell and tubes configuration as helically coiled counter flow heat exchanger are preferred to PCHE. However, there is high accord about the use of PCHE in S-CO_2 cycles for recuperators and eventually for heat sources and heat sink heat exchangers, mainly because of their good behavior under high pressure difference, very high effectiveness (close to 99%) and high compactness. So, Argonne National Laboratory (ANL) uses them in the STAR-LM, a Generation IV reactor [25]; Korean Atomic Research Institute (KAERI) has selected them for KALIMER-600, another Generation IV reactor [26]; and finally, a PCHE is included in other experimental helium loop developed by KAERI to test a design for a fusion reactor based on a helium cooled molten lithium (HCML) blanket [27]. A benchmarking survey with actual prototypes of reactors can be found in Refs. [28], with thermal effectiveness from 92 % to 98.7 %; SANDIA National Laboratory [29] supports their use for both recuperators, heat entry to the power cycle and heat rejection from the cycle, highlighting the benefits of PCHE compactness; Mito et al. [30] draw attention to the reduced pressure drop and Gezelius [31] gave ratios of 58–98 MW/m^3 for PCHE against 6.2 MW/m^3 with shell and tube heat exchangers working at the same capacity and log mean temperature difference. In Ref. [13] a detailed design of an S-CO_2 for 300 MW of mechanical power is given resulting minimum temperature approaches between 4 and 5 °C for both recuperators and precooler and power densities in the range of 7.7–13.4 MW/m^3 (the lowest at LTR and the highest at precooler). In addition, many authors have investigated the characteristics of hydraulic performance of a PCHE, experimentally and numerically. Nikitin [32] studied the performance of a PCHE with zigzag channels in a supercritical CO_2 experimental loop. Ngo et al. [33] analyzed a new PCHE with an S-shaped fin by using a heat recovery test facility, confirming a promising thermal-hydraulic performance with water and CO_2. And following these studies, Tsuzuki et al. [34] with a 3D model obtained a pressure drop reduction in a novel flow channel configuration with discontinuous fins with an S-shape. Then, Kim et al. [35] showed that airfoil shaped fin could suppress separation in the flow, which could improve the pressure drop reduction with respect to S-shaped fins. Other geometries have been analyzed in Kim et al. [36], with a longitudinal corrugation flow channel, and a modified fin structure to the previous work mentioned above is proposed in Xu et al. [37], which enhances flow resistance reduction. Another important issue regards the heat exchangers in fusion applications is the tritium permeation. In Ref. [38] a two dimensional finite element analysis is conducted to analyze this topic in PCHE for VHTR, assessing the effective thickness for tritium permeation. In Ref. [39] permeation in a new design of compact heat exchanger

for a fusion reactor using a DCLL blanket is analyzed, showing that when using silicon carbide as structural material the permeation is practically non-existent.

This paper focuses on the balance of plant for a fusion reactor based on an HCLL blanket. High thermal sources (blanket) and low ones (divertor and vacuum vessel) have been considered and eventually integrated in an S-CO_2 power cycle searching the maximization of the electricity production. A realistic estimate of electrical efficiency has been derived by accounting the pumping power demanded by the heating and cooling loops feeding the power cycle and even the self-consumptions of the plant. Once an optimum layout has been selected based on electricity production, the study has been completed by the optimization of the heat exchangers, so that a trade-off between heat exchangers size and power production has been proposed. In short, the technical feasibility of S-CO_2 for a DEMO fusion reactor based on HCLL has been assessed.

2. Thermal specification of the DEMO reactor

Fig. 1 shows a sketch of the balance of plant for the DEMO reactor. It is observed that the reactor supplies the heat to the power cycle from three different sources: blanket (BNK), divertor (DIV) and vacuum vessel (VV). Each source delivers different amounts of thermal power at different range of temperatures using its own cooling medium. So, blanket is cooled by helium and divertor and vacuum vessel by water in separate cooling loops. As in any power cycle there is an amount of heat released to the sink, shown in Fig. 1 by a water loop with a cooling tower. Each cooling loop requires a circulating device (circulator for helium and pump for water) which demands a pumping power from the gross electricity (W_{gross}) produced by the electric generator. Another electric consumption (W_{aux}) is required for both auxiliaries and the heating and current drive in the plasma where the fusion reaction occurs.

Thermal specifications of the DEMO reactor were described in the Work Programme 2013 for DEMO 1A reactor [4] and they are summarized in Table 1, which also includes estimations for parasite power consumptions (W_{aux}).

The thermal power given in Table 1 is the one absorbed by the cooling fluids in the reactor (Q_{BNK}, Q_{DIV} and Q_{VV}). To obtain the thermal power supplied to the power cycle ($Q_{BNK,cy}$, $Q_{DIV,cy}$ and $Q_{VV,cy}$) is necessary to add the pumping power. Pump isentropic efficiencies have been set to 82% for the blanket (circulator) and 85% for the divertor and the vacuum vessel; pressure loss through the in-reactor heat removal has been assumed to be 1% [40]. Regarding to the pumping power in the sink loop, the assumption given in Equation (1) has been done according to [40]:

$$W_{sink} = Q_{sink} \cdot \left(\frac{200\,kPa}{4.18\,kJ/(kg \cdot K) \cdot 5\,K \cdot 1000\,kg/m^3} \right) \approx 0.96\%\, Q_{sink} \qquad (1)$$

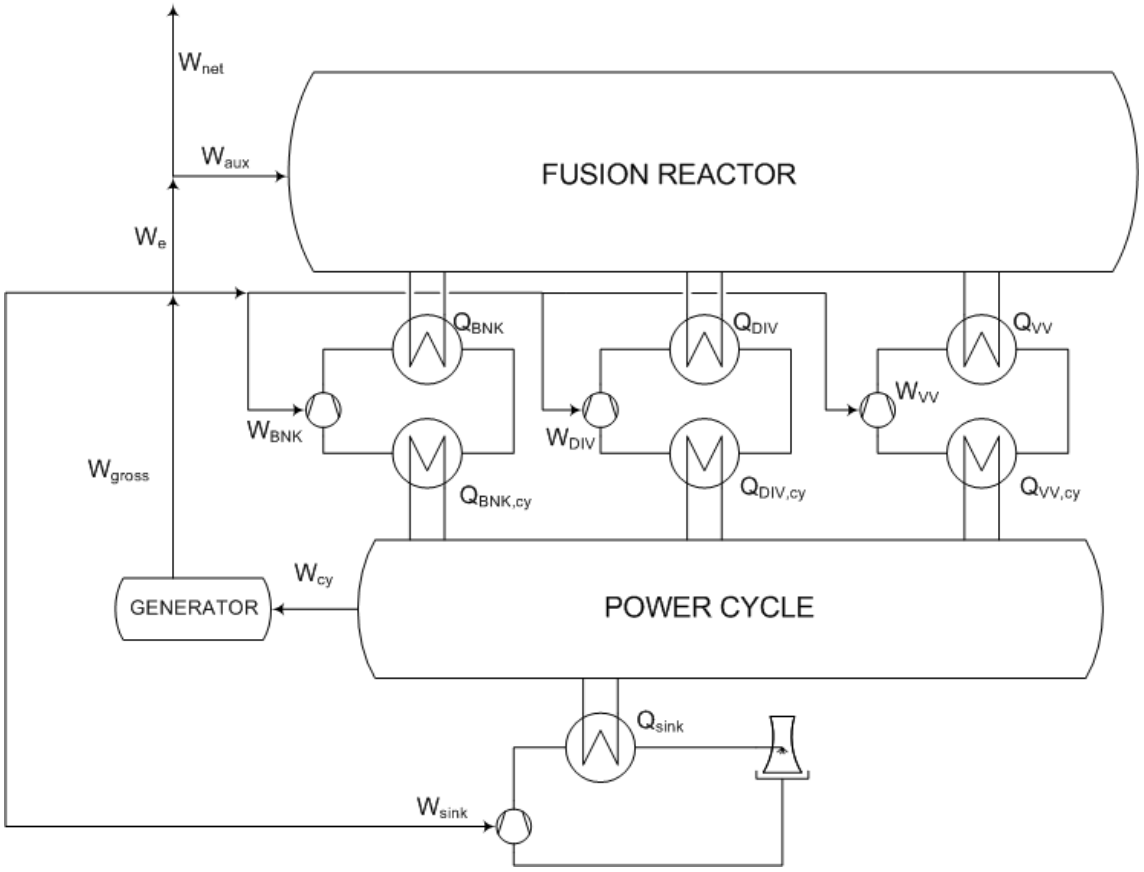

Fig. 1. Systems involved in the Balance of Plant.

Table 1. Specifications for DEMO 1A reactor (Source: [4]).

	Blanket	Divertor	Vacuum Vessel	Overall
Thermal Power (MW)	1835	149	34.56	
Inlet temperature Helium (ºC)	300			
Outlet temperature Helium (ºC)	500			
Outlet pressure Helium (bar)	80			
Helium pressure drop (bar)	4.35			
Inlet temperature Water (ºC)		150	95	
Outlet temperature Water (ºC)		250	105	
Outlet pressure Water (bar)		65	11	
Water pressure drop (bar)		2	1	
Power for auxiliaries (MW)				135
Power for H&CD (MW)				50
Net electrical power (MW)				≥ 500

3. Methodology

The classical assessment in thermodynamic power cycles is focused on the First Law, where the efficiency of the cycle involves the mechanical power produced by the cycle (W_{cy} in Fig. 1) and the heat delivered by the thermal source to the cycle ($Q_{x,cy}$ in Fig. 1, being "X" BNK, DIV and/or VV, depending of the considered scenario) [6]. The present study also includes the pumping consumption in both thermal sources and sink, the efficiency of the electric generator and other parasitic consumptions devoted to maintain the plasma conditions. This type of assessment has

been already performed by some authors in the steady-state operation of an SFR reactor [8] and by Floyd et al. [23] in the off-design. In both cases the heat transfer fluid in the thermal source was sodium, i.e., a liquid metal which is pumped (nearly incompressible). In the case of a fusion power plant with a HCLL blanket, the helium (compressible fluid) is responsible of the higher input of thermal power (more than 90% in Table 1) which demands a circulator to move it with a high electric demand (162 MW in Table 2). So, in feasibility studies of fusion power plants, a key issue is to take into account the pumping power. Another key issue, specific of fusion power plants, is the consideration of parasitic loads necessary to maintain the plasma conditions (185 MW in Table 1).

Table 2. Consumptions and state points at the cooling loops (notation according to Fig. 1. "x" denotes BNK, DIV or VV).

	Blanket	Divertor	Vacuum Vessel
Heat from reactor (Q_x) [MW]	1,835	149	34.56
Heat to cycle (Q_{xcy}) [MW]	1,997	149.1	34.67
Pumping consumption (W_x) [MW]	162	0.112	0.112
Reactor inlet temperature (IR) [ºC]	300	150	95
Reactor inlet pressure (IR) [bar]	84.35	67	12
Reactor outlet temperature [ºC]	500	250	105
Reactor outlet pressure [bar]	80	65	11
Pump/circulator inlet temperature [ºC]	282.7	150	94.99
Pump/circulator inlet pressure [bar]	79.2	64.4	10.9

Fig. 1 shows the different powers produced by the balance of plant, from the cycle to the bus bar of power plant. So, the mechanical power produced by the cycle (W_{cy}: the turbine minus the compressors) is converted into gross electric power (W_{gross}) by the electric generator through its generator efficiency (Equation (2)), fixed at 97% according to [40]:

$$\eta_g = \frac{W_{gross}}{W_{cy}} = 0.97 \tag{2}$$

The ratio of each power (cycle, gross, electric and net ones) to a reference input of heat defines the different efficiencies of the plant. In the case of cycle efficiency (η_{cy}) only the heat of the thermal source supplied to the thermodynamic cycle is taken into account (the heat from the blanket, $Q_{BNK,cy}$, is always supplied to the cycle, but in some scenarios the heat from divertor, $Q_{DIV,cy}$, and/or the vacuum vessel, $Q_{VV,cy}$, are directly released to the sink). In other cases (gross efficiency, η_{gross}, electric efficiency, η_e, and net efficiency, η_{net}) the reference heat is always the sum of the thermal power delivered by the reactor to each heat exchanger ($Q_{BNK} + Q_{DIV} + Q_{VV}$).

Fig. 2 shows a classical S-CO_2 layout which takes heat from a unique thermal source, the blanket. This layout is the baseline case and is denoted as Layout 0. Using this layout it is assumed that the rest of the thermal sources release their heat power directly to the sink. S-CO_2 is basically a recuperative Brayton cycle where the working fluid operates always at supercritical pressure, being the lower pressure close to the critical one. This fact allows reducing the compression power due to the high density of CO_2 at the compressor inlet but also complicates the recuperator performance. So, at low temperatures (70 °C–150 °C), the CO_2 specific heat is substantially higher at high pressure than at low one, which would entail to an unbalanced heat exchanger (the difference between the hot stream and the cold stream temperatures would not be constant) with the consequent reduction in effectiveness. This unbalance is overcome through splitting recuperation in two serial stages (Low Temperature Recuperator, LTR, for low temperature range and High Temperature Recuperator, HTR, for high temperature range), which allows that a fraction of the high pressure stream by-passes the LTR ("*x*" fraction in stream 6–9 in Fig. 2), introducing a new compressor (Auxiliary Compressor) which compresses this by-pass "*x*"

fraction. The fraction "*x*" is usually determined imposing the balance in the LTR heat exchanger (the same temperature difference at both extremes). This arrangement is the so called re-compression cycle (other arrangements to overcome the heat exchange drawback are feasible [9]).

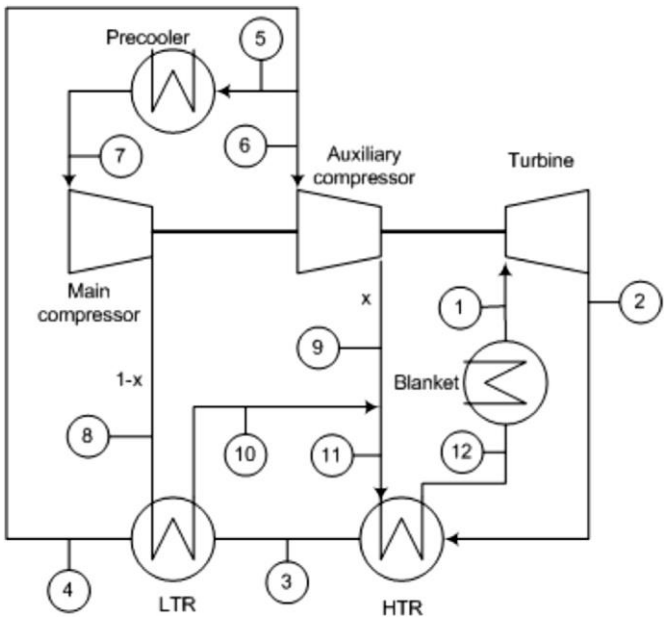

Fig. 2. Classical re-compression supercritical CO_2 Brayton cycle. This arrangement constitutes the Layout 0 (baseline case) at present study.

Another issue stemming from the CO_2 specific heat sharp changes at low temperature is that the minimum temperature difference between the two CO_2 streams (i.e., pinch point [41]) occurs inside the LTR (this issue also can occur in the precooler). This requires special attention when assessing LTR performance (a detailed Temperature vs. Heat Power transfer, *T*–*Q*, profile is needed for an accurate analysis). Fig. 3 shows the *T*–*Q* profiles on both recuperators of Layout 0. These have been obtained discretizing the heat exchangers and establishing an energy balance on each sub-heat exchanger. It is observed that the choice of the fraction by-passing the LTR ("*x*") allows achieving the balance of LTR, although the actual pinch point occurs inside the heat exchanger, being lower than the temperature difference achieved at the extremes. In the case of HTR the balance cannot be achieved (another re-compression would be necessary) but as the values of the specific heat are nearly constant (temperatures are separated enough from the critical one) the temperature profiles are straight lines, suffering the hot stream (lower pressure, so lower specific heat) the highest temperature variation (at HTR both streams have the same mass flow rate).

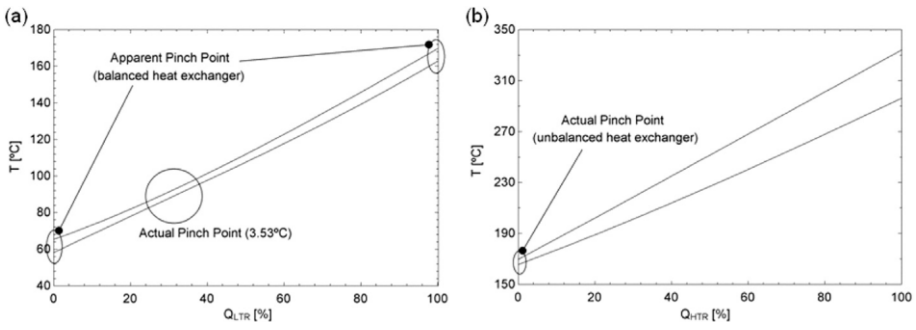

Fig. 3. Temperature vs. Heat Power exchanged at LTR (a) and HTR (b) in Layout 0.

As said above, the re-compression S-CO_2 power cycle has been chosen to explore its potential coupling to the HCLL DEMO reactor. Some authors [13] analyzed the convenience of the inclusion of the divertor as a thermal source. They investigated the reduction on cycle efficiency due to the low temperature of the divertor (no vacuum vessel was considered in Ref. [13]). Therefore, although the cycle efficiency decreases, the power produced by the cycle increases due to the higher power heat input. So, the analysis about the inclusion of divertor and vacuum vessel in the thermal sources, and even the study of their position in the layout to maximize the electricity production, has become a key issue. In this context, different scenarios have been considered beyond the baseline case named Layout 0 to accommodate the different thermal sources, hereafter named A, B, C and D (note that vacuum vessel is only included in scenarios C and D). Fig. 4 compiles all these layouts in a simplified manner and Table 3 shows the destination of the heat released by each thermal source in each layout. As noted, the blanket is always situated upstream the turbine, whereas the divertor and vacuum vessel locations depend on the scenario. The divertor is situated downstream the auxiliary compressor in Layout A, and by-passing the LTR in B, C and D. The vacuum vessel is upstream the divertor (at the same branch) in C and upstream the LTR in D.

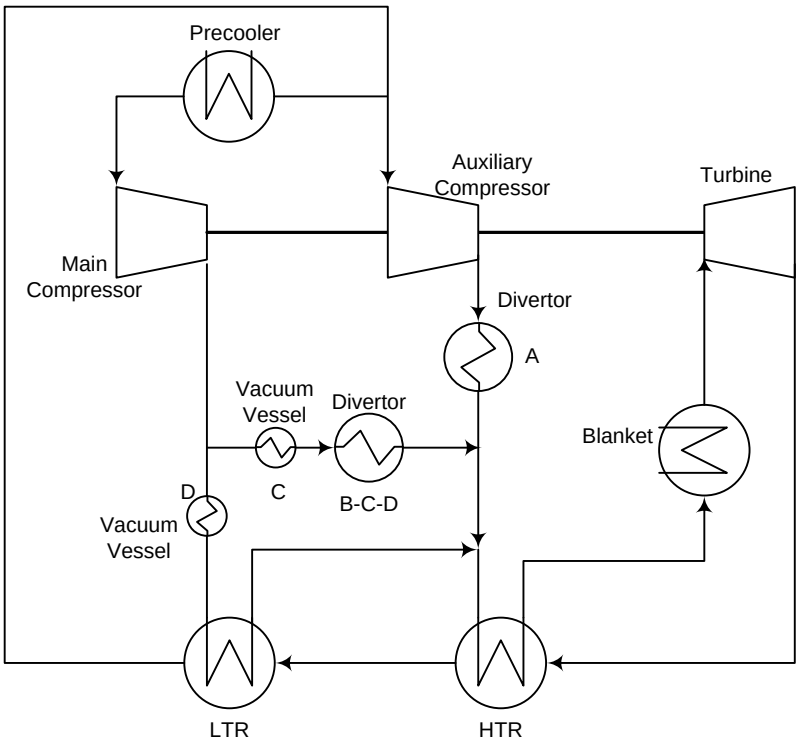

Fig. 4. Sketch of different layouts considered.

Table 3. Destination of the heat released by the thermal sources in each layout.

Layout	Blanket	Divertor	Vacuum Vessel
0	Power cycle	Sink	Sink
A	Power cycle	Power cycle	Sink
B	Power cycle	Power cycle	Sink
C	Power cycle	Power cycle	Power cycle
D	Power cycle	Power cycle	Power cycle

At the main compressor, conditions of 85 bar and 30 °C have been considered. The temperature is below the pseudo-critical point, but possible stability problems are prevented with the chosen pressure, far enough from the critical one to smooth the density–temperature curve as explained

in Ref. [10]. Inlet auxiliary compressor pressure is 85.4 bar and the value at the LTR outlet is temperature dependent.

In all the layouts, except Layout A, CO_2 enters the turbine at 280 bar and around 447 °C. This pressure matches the usual pressure ratio in S-CO_2 cycles (250/75) [7], with the low pressure set at 85 bar. McDonald [42] chose 241 bar as a typical value for the inlet pressure in a steam turbine of a supercritical cycle for a nuclear power plant based on a combined cycle, using a VHTR reactor for topping cycle. Floyd et al. [23] stated 250 bar as a conservative value due to its compatibility with commercial pipes while Weitzel [43] fixed the present technology status (ultra-supercritical steam turbines) between 260 and 270 bar, being the limits (necessary to implement CO_2 capture technologies at reasonable costs of electricity) from 310 to 380 bar according to steam turbine manufacturers. So, 280 bar has been chosen as a compromise solution between well-established and medium-term technology, being closer to the former. Temperature is the maximum allowed for an acceptable value of the pinch point in the blanket heat exchanger. In Layout A, limitations from the divertor force to reduce the high pressure value to 230 bar and 417.8 °C. In the literature about S-CO_2 cycle modeling there are well established ranges for adiabatic efficiencies of turbomachinery [16]. So, efficiency for compressors varies from 75% [14], passing by 87.5% [26] to 95.5% [7]. A value of 88% has been taken for the present study. Regards to the turbine, the efficiency varies from 92.9% [7], passing by 93% [14] to 93.4% [26]. A value of 93% has been taken for the present study.

The entropy generation rate is used as a measurement of the internal irreversibility in the recuperators. In an adiabatic heat exchanger the general expression is given by Equation (3):

$$S_{gen.HX} = m_h(s_{ho} - s_{hi}) + m_c(s_{co} - s_{ci}) \quad (3)$$

where "*h*" denotes hot stream, "*c*" cold one, "*i*" the input port and "*o*" the output one.

In order to achieve high efficiency, low pinch points have been chosen. So, in all the cases but LTR, the range is set to 4 °C ÷ 5 °C. In LTR the minimum temperature difference (defined at the extremes of the heat exchanger) has been set to 7 °C in order to achieve an actual pinch point inside the heat exchanger higher than 3 °C. All these pinch point values are compatible with PCHE [13]. Pressure drops in the heat exchangers were assumed to be 40 kPa and no pressure loss is assumed along pipes and ducts [44].

In all the scenarios, the heat exchangers have been discretized in sub-heat exchangers using suitable correlations [45]. Pressure drop and energy conservation equations are solved iteratively. At each time step, heat transfer coefficients are derived and, through the Log Mean Temperature Difference (LMTD) method [41], the heat exchanger length is estimated. In case the pressure drop condition is not satisfied, the number of channels is changed and the whole iterative process is initiated again. At the end of the calculation, the cross-section surface area and volume are calculated. Finally, it is verified that the number of channels and their length per module (0.6×0.6 m^2) do not exceed the current manufacturing capability (96,000 and 1.5 m, respectively) [45].

4. Results

4.1. Comparison of layouts

Table 4 summarizes the electric power (W_e) and efficiency (η_e) achieved with the different layouts investigated. These parameters have been chosen because they take into account pumping consumption and leave out the auxiliaries consumption, whose power requirements are still highly uncertain at this stage of the DEMO reactor design.

Table 4. Electric power and efficiency with investigated layouts.

Layout	Power [MW]	Efficiency [%]
0	650.1	32.20
A	662.6	32.82

B	677.6	33.57
C	684.0	33.89
D	675.8	33.48

The inclusion of the divertor in the BoP increases thermal efficiency between 2 and 4%, roughly, with respect to the basic Layout 0. The additional inclusion of the vacuum vessel entails a slightly higher improvement (between 4 and 5%, approximately). By comparing layout B (no vacuum vessel) with C and D, the significance of a right integration of thermal sources is noticeable: whereas including vacuum vessel even worsens the cycle thermal performance in case D, it is improved in case C, although in none of the cases the effect is too significant, as expected.

4.2 Selected layout

Table 4 highlights that layout C shows the best electrical performance and in Fig. 5 the *T–s* diagram of the cycle is represented, showing the state points (Table 5). This means that when working in series with the divertor, the low flow rate (822 kg/s) of CO_2 heated up within the vacuum vessel heat exchanger makes the divertor more effective. As a result, the mixing of this stream and the one coming from the auxiliary compressor makes heat absorption at the HTR more efficient and also optimizes, to some extent, the thermal state of CO_2 at the inlet of the blanket.

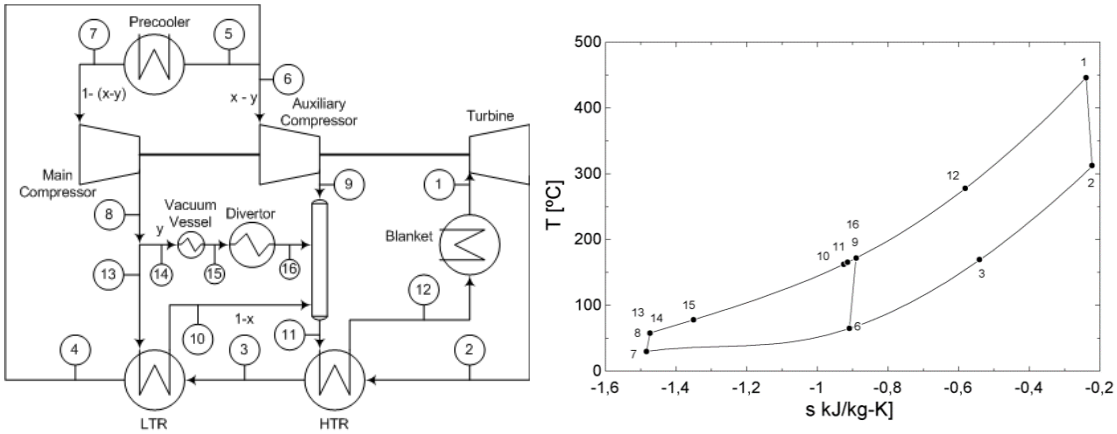

Fig. 5. Selected layout C: arrangement of components (left); T-s diagram at design point (right).

Table 5. State points of selected layout C (notation according to Fig. 5 left).

	P [bar]	T [ºC]	h [kJ/kg]	s [kJ/kg·K]		P [bar]	T [ºC]	h [kJ/kg]	s [kJ/kg·K]
1	280.0	446.5	392.9	-0.2397	9	280.8	172.2	24.51	-0.8909
2	86.20	313.0	259.4	-0.2224	10	280.4	162.9	9.022	-0.9258
3	85.80	169.9	95.82	-0.5416	11	280.8	165.9	13.95	-0.9148
4	85.40	65.20	-46.11	-0.9100	12	280.4	278.0	177.5	-0.5814
5	85.40	65.20	-46.11	-0.9100	13	281.2	58.20	-199.0	-1.4743
6	85.40	65.20	-46.11	-0.9100	14	281.2	58.20	-199.0	-1.4743
7	85.00	30.00	-227.4	-1.4846	15	280.8	78.35	-156.8	-1.3506
8	281.2	58.20	-199.0	-1.4743	16	280.4	172.2	24.62	-0.8904

Table 6 characterizes the turbomachinery performance. As expected, using CO_2 as the working fluid substantially reduces power consumption with respect to a classical Helium Brayton cycle. The apparently high value of power required by the auxiliary compressor, despite the low flow rate passing through (comparable to the main compressor one), is due to the higher temperature of the not-precooled CO_2 stream, which makes its density lower.

Table 6. Performance of turbomachines in Layout C.

	Turbine	Main Compressor	Auxiliary Compressor
Mass flow rate [kg/s]	9271	7,49	2122
Power [MW]	1238	202.9	149.9

Table 7 compiles the heat exchangers performance and the pumping consumption. The power corresponding to blanket, divertor, and vacuum vessel is the one entering the cycle (i.e., once circulator (He) or pump (water) consumptions are included). It is seen the effectiveness reaches two different set of values: higher than 93% in blanket, LTR, and HTR and lower than 59% in divertor and vacuum vessel. This fact is a consequence of the different pinch points in each of the heat exchangers (lower than 5 °C in the former and higher than 26 °C in the latter). So, in the former group the pinch point has been set to a low value to achieve a high efficiency in the cycle, while in the latter one the pinch point is determined by the rest of imposed conditions, which avoid low values.

Table 7. Performance of heat exchangers and power consumption in pumping in Layout C. ([a]The pinch point is related to precooler heat exchanger water/CO2; [b]The consumption is related to the pumping in water loop.)

	Blanket	Divertor	V. Vessel	LTR	HTR	Sink
Power [MW]	1,997	149.1	34.67	1,316	1,516	1,296
Pinch Point [ºC]	4.7	71.65	26.65	3.5	4	5[a]
Efectiveness [%]	97.87	58.27	43.04	93.73	97.28	---
Consumptions [MW]	162	0.112	0.112	---	---	12.4[b]

Table 8 shows the size of all the heat exchangers used in Layout C together with their volumetric specific power. Divertor and vacuum vessel heat exchangers exhibit the highest volumetric specific power due to their high pinch point, whereas LTR has the lowest one as its pinch point is the smallest one. Blanket, precooler and HTR have similar specific power due to their similar pinch points and all of them are slightly unbalanced, although HTR requires more surface area, as both heat exchanger streams are CO_2 (in the other cases, water and He, which are better cooling fluids, flow through the primary side of the component).

Table 8. Sizes of the heat exchangers at the design point.

	Frontal area [m^2]	Length [m]	Volume [m^3]	Specific power [MW/m^3]
Blanket	64.35	1.53	98.4	20.29
Divertor	1.76	0.34	0.60	249.9
V. Vessel	1.96	0.16	0.31	111.6
LTR	141.5	4.26	603.2	2.18
HTR	101.3	1.48	149.8	10.1
Precooler	96.75	0.59	57.12	22.69

Finally, Table 9 shows the detailed performance of Layout C. As observed, even though power cycles can reach reasonable values of thermal efficiencies and power, fusion reactors will face with two major drawbacks: the cooling power needed for blanket, divertor, and vacuum vessel (gross to electric performances) and, no less important, the power demanded by all the reactor auxiliaries (electric to net performances).

Table 9. Power and efficiencies in Layout C.

	Cycle	Gross	Electric	Net
Power [MW]	885.2	858.7	684.0	499.0
Efficiency [%]	40.59	42.54	33.89	24.72

4.3 Sensitivity analysis

A sensitivity analysis to explore which components affect the whole cycle configuration more strongly has been carried out. The studied variables have been: the heat exchanger size (measured by the pinch point) and their pressure drop, also the turbine inlet pressure and the main compressor inlet temperature. In short, both heat exchangers and turbomachinery performance have been studied. The insights from this study might be valuable for cycle cost optimization.

Fig. 6 summarizes the influence of the chosen variables in gross power (i.e., no effect of pumping consumption is accounted for in the analysis) by means of the percentage variation of the gross power when each variable varies 1%. As noted in Fig. 6, any need of pinch point increase might be compensated by raising the pressure at the turbine inlet or by reducing the inlet temperature at the main compressor. However, the latter is rejected because of the limitations imposed by the heat sink temperature.

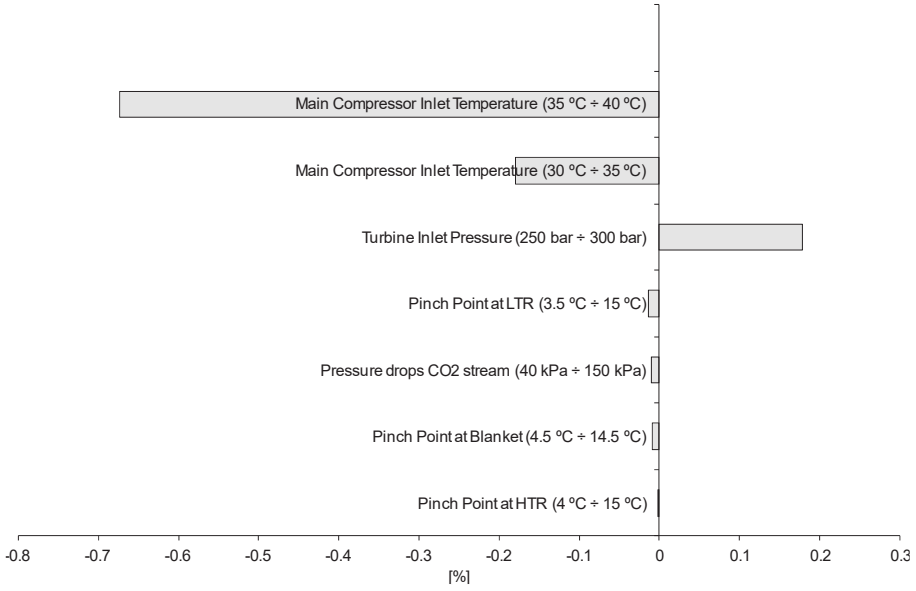

Fig. 6. Sensitivity of gross power to 1% of change in key variables.

The results indicate that the precooler is the most important heat exchanger. A high temperature at the inlet of the main compressor would burden gross power so substantially that precooler performance turns out to be instrumental for the cycle. Then, the second more important heat exchanger is the LTR, followed by the blanket. So, it is necessary to set the pinch points as low as possible in order to maximize the power generation which entails to the choice of PCHE due to its excellent performance on high effectiveness (low pinch points) and relative compactness. From Fig. 6 it is also derived the low influence in the gross power of the pinch point at HTR. This result, apparently contrary to Sarkar's conclusions [11] who established that the HTR has more influence than the LTR in the efficiency of the cycle, can be better understood through a Second Law analysis.

Fig. 7 shows the *T*–*Q* profile at HTR and LTR depending on the pinch point considered. It is observed that the effect of increasing the pinch point is to increase the temperature difference of both streams. However, while at LTR this entails a nearly constant separation since this heat exchanger is designed to be balanced, at HTR the larger temperature difference reduces the level

of unbalance of the heat exchanger, which makes gross power drop smaller. This behavior is also revealed by the Second Law analysis shown in Fig. 8, which shows higher irreversibilities at HTR than at LTR. However, the increase of the pinch point at LTR makes its irreversibilities grow in 239% while this is restricted to just 8.8% at HTR. On the other hand, the increase of the pinch point at HTR even reduces its irreversibilities in 6.7% while it would take the LTR to levels of around 36.4%. In short, the irreversibility in both recuperators rises to 47% when pinch point at LTR increases but only to 5.9% when is the HTR pinch point the one that increases. That is, at a given point of operation the HTR taxes more heavily the power output of the cycle than the LTR, due to its higher irreversibilities (as stated in Ref. [11]). However, the internal heat exchangers *T*–*Q* profiles make the sensitivity of the power output to the pinch point in both recuperators be much higher at LTR than at HTR.

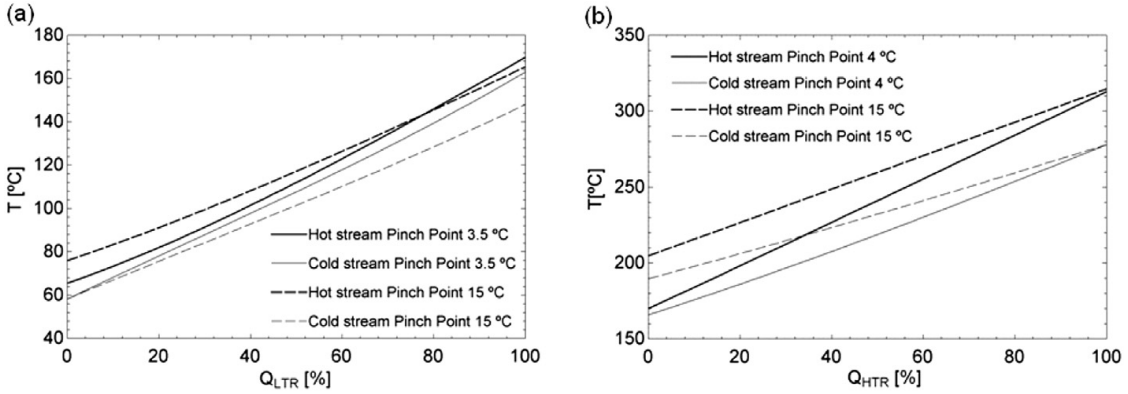

Fig. 7. T-Q profiles at LTR (a) and HTR (b).

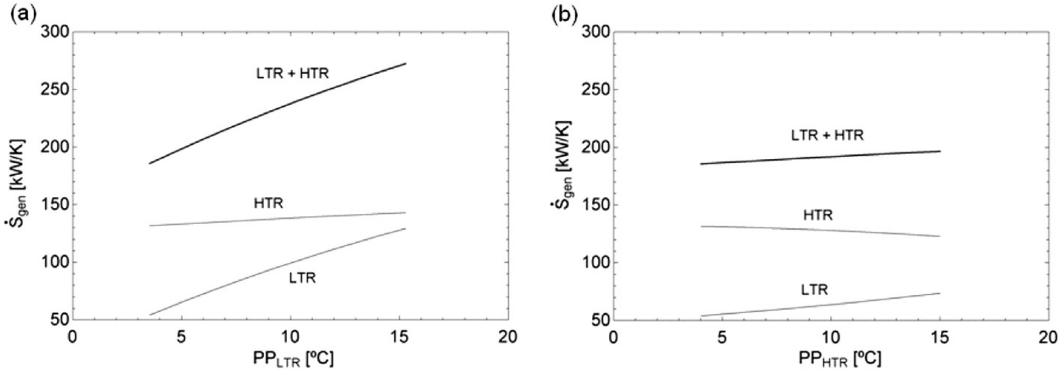

Fig. 8. Entropy generation rate at both recuperators depending on the pinch point at LTR (a) and HTR (b).

Taking into account the results from the sensitivity analysis, Table 10 summarizes the parameters set of what has been called the Layout C-ECO. It may be noted that the main compressor inlet temperature has not been changed as it cannot be further reduced. All the pinch points have been increased (the highest increase has been set at the HTR because it hardly affects the cycle performance). Pressure drops have been also increased, so that the heat exchangers size can be reduced. And, finally, the turbine inlet pressure has been increased to compensate the reduction in gross power due to the increment in pinch points.

Table 10. Key parameters of Layout C-ECO scenario

Turbine inlet pressure [bar]	300
Main compressor inlet temperature [ºC]	30
Pressure drops at CO_2 streams [kPa]	60
Pinch Point at Blanket [K]	7.7
Pinch Point at HTR [K]	10
Pinch Point at LTR [K]	5

Table 11, Table 12, Table 13 fully characterize this new layout C-ECO, as done above with all the other layouts explored. Table 11 gathers the performance in turbomachinery, with an increase of 1% in the turbine power and a 5% in the compressor consumption. Table 12 compiles the performance at the heat exchangers; all the effectiveness values fall except at divertor and vacuum vessel, as in these heat exchangers the pinch points were reduced as a consequence of the key parameter changes. Table 13 gives the size of the heat exchangers in the Layout C-ECO: whereas divertor and vacuum vessel increase slightly due to the reduction of their pinch points, the largest heat exchangers become smaller (19% at blanket, 32% at LTR, 57% at HTR); no significant change has been found in the precooler.

Table 11. Performance of turbomachines in Layout C-ECO.

	Turbine	Main Compressor	Auxiliary Compressor
Mass flow rate [kg/s]	8911	6926	1985
Power [MW]	1250	216.0	155.4

Table 12. Performance of heat exchangers and power consumption in pumping in Layout C-ECO. ([a]The pinch point is related to precooler heat exchanger water/CO2; [b]The consumption is related to the pumping in water loop.)

	Blanket	Divertor	V. Vessel	LTR	HTR	Sink
Power [MW]	1,997	149.1	34.67	1494	1118	1,302
Pinch Point [ºC]	7.7	65.55	22.79	5.64	10	5[a]
Efectiveness [%]	96.56	60.93	48.85	93.82	91.68	---
Consumptions [MW]	162	0.112	0.112	---	---	12.5[b]

Table 13. Sizes of heat exchangers at economic point.

	Frontal area [m^2]	Length [m]	Volume [m^3]	Specific power [MW/m^3]
Blanket	58.95	1.35	79.8	25.02
Divertor	1.51	0.40	0.608	245.11
V. Vessel	2.09	0.18	0.372	93.27
LTR	108	3.78	408.4	3.69
HTR	64.57	0.98	64.57	17.25
Precooler	96.75	0.59	57.06	22.78

Finally, Table 14 summarizes the performance of Layout C-ECO. Compared to the original Layout C, a very slight decrease of electric efficiency charges the economic design and, in terms of net power, it hardly means a 1% reduction. Therefore, the C-ECO design would be the most promising configuration among those explored in the present work, since despite having a minor effect on power cycle performance, it would mean a reduction of around 35% in the global volume of the heat exchangers, which would be likely worth.

Table 14. Power and efficiencies in Layout C-eco.

	Cycle	Gross	Electric	Net
Power [MW]	878.86	852.49	677.77	492.8
Efficiency [%]	40.30	42.23	33.58	24.41

5. Conclusions

This paper presents an exploratory study carried out under the framework of the EFDA Work Program 2013 to analyze the technical feasibility of using S-CO_2 power cycles for low-temperature divertor fusion reactors, such as it was proposed in Ref. [4]: three thermal sources, in which the blanket, cooled by Helium, is dominant. Potential strengths and weaknesses have been discussed based on the open literature produced under conditions close enough to the ones here explored. Through a conventional methodology based on the First and Second Laws of Thermodynamics and with a number of approximations and hypothesis made, four alternatives to a basic cycle in which the blanket is the only thermal source have been proposed and investigated. The main insights withdrawn from the results might be summarized as follows:

- Electric power and efficiency have been improved more than 5% from the baseline scenario (i.e., only blanket feeding the power cycle) matching in a proper way all the available thermal sources.
- The configuration selected, with better output, is the one with vacuum vessel and divertor located in series in the bypass line of the LTR, after the main compression. This arrangement achieves 885.2 MW of cycle power and 40.6% of cycle efficiency.
- The pumping power (in both thermal sources and sink) and the parasitic loads have been included in the performance assessment, entailing to high taxes due to helium is the main heat transfer fluid. So, the power produced by the electric generator is reduced a 20% after covering the pumping power and another 27% after feeding the demand for auxiliaries, heating and current drive, achieving a net efficiency of 24.7%.
- A sensitivity study has identified the turbine inlet pressure and the main compressor inlet temperature as the key variables in the performance of the plant. Regarding the heat exchangers the pinch point at LTR and the overall pressure drop are the most influential variables. Their increase, according to their influence on electricity production, means a reduction of 1/3 of the overall volume of the heat exchangers. The turbine inlet pressure has been increased 20 bar to maintain the power losses below 1%.

As DEMO operational parameters are being assessed from different perspectives, it is highly likely that the final ones will differ from the ones used in this work. Nonetheless, the potential of S-CO_2 cycles as suitable converters of thermal energy to power, the significance of a suitable integration of thermal sources to maximize the electrical output and the identification of the key components of the layout as a way to optimize the whole cycle performance have been discussed based on a generic methodology that would be applicable to any other fusion reactor settings.

Acknowledgement

Authors acknowledge to EFDA consortium in their activities of 2013 the funding of the Task WP13-DAS-08-T02: *Design, modeling and analysis of primary heat transfer and BoP options for integration with a DEMO fusion power plant*, in which frame this paper has been developed.

References

[1] F. Romanelli, Fusion Electricity: A Roadmap to the Realization of Fusion Energy, EFDA, November 2012, ISBN 978-3-00-040720-8.

[2] L.V. Boccaccini, A. Aiello, O. Bede, F. Cismondi, L. Kosek, T. Ilkei, J.-F. Salavy, P. Sardain, L. Sedano, European TBM Consortium of Associates, Present status of the conceptual design of the EU test blanket systems, Fusion Eng. Des. 86 (2011) 478e483.

[3] D. Maisonnier, et al., A Conceptual Study of Commercial Fusion Power Plants, April 13th, 2005. Final Report of the European Fusion Power Plant Conceptual Study (PPCS), EFDA-RP-RE-5.0.

[4] J. Harman, EFDA Work Programme 2013, Design Assessment Studies, Technical Specification, WP13eDAS08: Primary Heat Transfer & Balance of Plant Systems, 2013. EFDA_D_2LJB2E v2.3. Specifications for WP13-DAS08-BOP.

[5] L.E. Herranz, J.I. Linares, B.Y. Moratilla, Power cycle assessment of nuclear high temperature gas-cooled reactors, Appl. Therm. Eng. 29 (2009) 1759e1765.

[6] J.I. Linares, L.E. Herranz, B.Y. Moratilla, I.P. Serrano, Power conversion systems based on Brayton cycles for fusion reactors, Fusion Eng. Des. 86 (2011) 2735e2738.

[7] V. Dostal, A Supercritical Carbon Dioxide Cycle for Next Generation Nuclear Reactors, Massachusetts Institute of Technology, USA, 2004 (Ph.D. thesis).

[8] G.D. Pérez-Pichel, J.I. Linares, L.E. Herranz, B.Y. Moratilla, Thermal analysis of supercritical CO_2 power cycles: assessment of their suitability to the forthcoming sodium fast reactors, Nucl. Eng. Des. 250 (2012) 23e34.

[9] V. Dostal, M. Kulhanek, Research on the supercritical carbon dioxide cycles in the Czech Republic, in: S-CO2 Power Cycle Symposium 2009, RPI, Troy, NY, USA, April 29-30, 2009

[10] A. Moisseytsev, J.J. Sienicki, Investigation of alternative layouts for the supercritical carbon dioxide Brayton cycle for a sodium-cooled fast reactor, Nucl. Eng. Des. 239 (2009) 1362e1371.
[11] J. Sarkar, Second law analysis of supercritical CO2 recompression Brayton cycle, Energy 34 (2009) 1172e1178.
[12] W.S. Jeong, Y.H. Jeong, Performance of supercritical Brayton cycle using CO2- based binary mixture at varying critical pints for SFR applications, Nucl. Eng. Des. 262 (2013) 12e20.
[13] S. Ishiyama, Y. Muto, Y. Kato, S. Nishio, T. Hayashi, Y. Nomoto, Study of steam, helium and supercritical CO2 turbine power generations in prototype fusion power reactor, Prog. Nucl. Energy 50 (2008) 325e332.
[14] S.A. Wright, R.F. Radel, M.E. Vermon, G.E. Rochau, P.S. Pickard, Operation and Analysis of a Supercritical CO2 Brayton Cycle, 2010. SANDIA REPORT, USA, SAND2010e0171.
[15] R. Fuller, J. Noall, J. Preuss, Turbomachinery for supercritical CO2 power cycles, GT2012, in: Proceedings of the ASME Turbo Expo 2012, July 17e20, 2012. Copenhagen, Denmark (paper 25385).
[16] J.S. Bahamonde-Noriega, Design Method for SeCO2 Gas Turbine Power Plants, Delft University of Technology, The Netherlands, 2012 (MSc Dissertation).
[17] L. Martín, M. Martín, Optimal year-round operation of a concentrated solar energy plant in the south of Europe, Appl. Therm. Eng. 59 (2013) 627e633.
[18] Z. Ma, C.S. Turchi, Advanced supercritical carbon dioxide power cycle configurations for use in concetrating solar power systems, in: Supercritical CO2 Power Cycle Symposium, Boulder, Colorado, USA, May 24-25, 2011. NREL/CP- 5500-50787.
[19] R. Chacartegui, J.M. Muñoz de Escalona, D. Sánchez, B. Monje, T. Sánchez, Alternative cycles based on carbon dioxide for central receiver solar power plants, Appl. Therm. Eng. 31 (2011) 872e879.
[20] C. Turchi, T. Held, J. Pasch, K. Gawlik, 10-MW Supercritical-CO_2 Turbine Test, SunShot Concentrating Solar Power Program Review 2013, April 23-25, 2013. Phoenix, Arizona, USA.
[21] B.D. Iverson, T.M. Conboy, J.J. Pasch, A.M. Kruizenga, Supercritical CO_2 Brayton cycles for solar-thermal energy, Appl. Energy 111 (2013) 957e970.
[22] R. Singh, S.A. Miller, A.S. Rowlands, P.A. Jacobs, Dynamic characteristics of a direct-heated supercritical carbon-dioxide Brayton cycle in solar thermal power plant, Energy 50 (2013) 194e204.
[23] J. Floyd, N. Alpy, A. Moisseytsev, D. Haubensack, G. Rodriguez, J. Sienicki, G. Avakian, A numerical investigation of the sCO_2 recompression cycle off- design behavior, coupled to a sodium cooled fast reactor, for seasonal varia- tion in the heat sink temperature, Nucl. Eng. Des. 260 (2013) 78e92.
[24] D. Aquaro, M. Pieve, High temperature heat exchangers for power plants: performance of advanced metallic recuperators, Appl. Therm. Eng. 27 (2007) 389e400.
[25] H. Song, Investigations of a Printed Circuit Heat Exchanger for Supercritical CO_2 and Water, Kansas State University, USA, 2007 (MSc Dissertation).
[26] J.E. Cha, T.H. Lee, J.H. Eoh, S.H. Seong, S.O. Kim, D.E. Kim, M.H. Kim, T.W. Kim, K.Y. Suh, Development of supercritical CO_2 Brayton Energy conversion system coupled with a sodium cooled fast reactor, Nucl. Eng. Technol. 41 (2009) 1025e1044.
[27] S.B. Yum, E.H. Lee, D.W. Lee, G.Ch. Park, Model validation of GAMMA code with heat transfer experiment for KO TBM in ITER, Fusion Eng. Des. 88 (2013) 716e720.
[28] B. Halimi, K.Y. Suh, Computational analysis of supercritical CO2 Brayton cycle power conversion system for fusion reactor, Energy Convers. Manage. 63 (2012) 38e43.
[29] S.A. Wright, R.F. Radel, R. Fuller, Engineering performance of supercritical CO2 Brayton cycles, in: ICAPP 10, San Diego, USA, June 13e17, 2010 paper 10264.
[30] M. Mito, N. Yoshioka, Y. Ohkubo, N. Tsuzuki, Y. Kato, Fast reactor with indirect cycle system of supercritical CO_2 gas turbine plant, in: ICAPP 06, Reno, Nevada, USA, June 4e8, 2006 paper 6265.

[31] K. Gezelius, Designs of Compact Intermediate Heat Exchangers for Gas Cooled Fast Reactors, Massachusetts Institute of Technology, USA, 2004 (MSc Dissertation).
[32] K. Nikitin, Y. Kato, L. Ngo, Printed circuit heat exchanger thermal-hydraulic performance in supercritical CO_2 experimental loop, Int. J. Refrig. 29 (2006) 807e814.
[33] T.L. Ngo, Y. Kato, K. Nikitin, N. Tsuzuki, New printed circuit heat exchanger with S-shaped fins for hot water supplier, Exp. Therm. fluid Sci. 30 (2006) 811e819.
[34] N. Tsuzuki, Y. Kato, T. Ishiduka, High performance printed circuit heat exchanger, Appl. Therm. Eng. 27 (2007) 1702e1707.
[35] D.E. Kim, M.H. Kim, J.E. Cha, S.O. Kim, Numerical investigation on thermal-hydraulic performance of new printed circuit heat exchanger model, Nucl. Eng. Des. 238 (2008) 3269e3276.
[36] J.H. Kim, S. Baek, S. Jeong, J. Jung, Hydraulic performance of a microchannel PCHE, Appl. Therm. Eng. 30 (2010) 2157e2162.
[37] X. Xu, T. Ma, L. Li, M. Zeng, Y. Chen, Y. Huang, Q. Wang, Optimization of fin arrangement and channel configuration in an airfoil fin PCHE for supercritical CO2 cycle, Appl. Therm. Eng. 70 (2014) 867e875.
[38] C. Oh, E. Kim, Heat Exchanger Design Options and Tritium Transport Study for the VHTR System, 2008. Idaho National Laboratory Report INL/EXT- 08e14799, USA.
[39] Fernández, L. Sedano, Design analysis of a lead lithium/supercritical CO_2 printed circuit heat exchanger for primary power recovery, Fusion Eng. Des. 88 (2013) 2427e2430.
[40] M. Porton, V. Vizvary, H. Latham, P. Clarkson, EFDA Work Programme 2012. Design Assessment Studies, 2012. WP12-DAS-08. EFDA_D_2M4XFP, v.1.0.
[41] J.E. Hesselgreaves, Compact Heat Exchangers. Selection, Design and Operation, Pergamon, Amsterdam, The Netherlands, 2001.
[42] C.F. McDonald, Power conversion system considerations for a high efficiency small modular nuclear gas turbine combined cycle power plant concept (NGTCC), Appl. Therm. Eng. 73 (2014) 80e101.
[43] P.S. Weitzel, Steam generator for advanced ultra-supercritical power plants 700 to 760C, in: ASME 2011 Power Conference, Denver, USA, July 12e14, 2011. BR-1852.
[44] M. Medrano, D. Puente, E. Arenaza, B. Herrazti, A. Paule, B. Brañas, A. Orden, M. Domínguez, R. Stainsby, D. Maisonnier, P. Sardain, Power conversion cycles study for He-cooled reactor concepts for DEMO, Fusion Eng. Des. 82 (2007) 2689e2695.
[45] I.P. Serrano, A. Cantizano, J.I. Linares, B.Y. Moratilla, Modeling and sizing of the heat exchangers of a new supercritical CO2 Brayton power cycle for energy conversion for fusion reactors, Fusion Eng. Des. 89 (2014) 1905e1908.

Acronyms

2D: two dimensional
ANL: Argonne National Laboratory
BNK: blanket
BoP: balance of plant
CSP: concentrated solar power
DCLL: Dual Cooled Lithium Lead blanket
DEMO: demonstration power plant
DIV: divertor
EFDA: European Fusion Development Agreement
HCLL: Helium Cooled Lithium Lead blanket
HCML: Helium Cooled Molten Lithium blanket
HTR: high temperature recuperator
ITER: International Tokamak Experimental Reactor
KAERI: Korean Atomic Energy Research Institute
KALIMER: Korean Advanced Liquid Metal Reactor
LMTD: log mean temperature difference
LTR: low temperature recuperator

PCHE: printed circuit heat exchanger
SCLL: Self Cooled Lithium Lead blanket
S-CO_2: supercritical CO_2 Brayton power cycle
SFR: sodium fast reactor
SNL: Sandia National Laboratory
STAR-LM: secure, transportable, autonomous reactor e liquid metal variant
TES: thermal energy storage
TeQ: temperature vs. heat power profile
VHTR: very high temperature reactor
VV: vacuum vessel
WCLL: Water Cooled Lithium Lead blanket

Notation

Letters
η: efficiency
Q: thermal power
W: power (consumed or generated)
m: mass flow rate
s: specific entropy
S: rate of entropy generation

Subscripts
BNK: blanket
c: cold
cy: cycle
DIV: divertor
e: electric
g: generator
gen: generated (referred to entropy generation rate)
gross: gross
h: hot
HX: heat exchanger
i input
net: net
o: output
sink: sink
VV: vacuum vessel